Pharmaceutical Sciences Asia

Pharm Sci Asia 2026; 53(3), 368-381

DOI:10.29090/psa.2026.03.26.9363

Research Article

Ternary-structured chitosan-stabilized nanoemulsions of *Plectranthus amboinicus* essential oil for enhanced antimicrobial performance in biomaterial applications

Khanh Ngoc Le[1], Dang Le Hai Hoang[2], Quang The Nguyen[2], Thanh Tien Nguyen[2], Anh Nam La[2], Dung Phuoc Tran Nguyen[3], Ngan Bao Hoang[2], Quynh Nhu Thi Nguyen[1], Nhung Mai-Hong Nguyen[4], Bao Ngoc Tran[4]*

[1] Hanoi University of Pharmacy, Faculty of Biotechnology, Hanoi, Vietnam
[2] Hanoi – Amsterdam High School for the Gifted, Hanoi, Vietnam
[3] Vietnam National University Hanoi, Hanoi, High School for Gifted Students, Hanoi, Vietnam
[4] Hanoi University of Pharmacy, Faculty of Pharmaceutics-Pharmaceutical Technology, Hanoi, Vietnam

ABSTRACT

Plectranthus amboinicus essential oil (PAEO) is known for its antimicrobial activity; however, its hydrophobfic nature limits its dispersion and consistency in aqueous environments. This study proposed PAEO-loaded nanoemulsions using a ternary phase system composed of Tween 80, phosphate buffer (pH 7.4), and chitosan to overcome this limitation. The ternary diagram exhibited a homogeneous region corresponding to nanoscale formulations and indicated that Tween and chitosan contribute to the stabilization of the emulsion system. The addition of caprylocaproyl polyoxyl-8 glycerides (Labrasol) to phosphate buffer (pH 7.4) expanded the homogeneous area, indicating improved formulation flexibility. Compared with pure PAEO, all nanoemulsion formulations significantly reduced MIC and MBC values ($p < 0.01$). Chitosan-containing formulations (F1-4 and F2-4) exhibited the highest antimicrobial activity, achieving >99.9% microbial reduction within 30 s against *Staphylococcus aureus*, *Escherichia coli*, and *Candida albicans*. The results indicate that chitosan was the primary factor responsible for the enhanced antimicrobial performance, whereas Labrasol mainly improved physicochemical stability. The combination of PAEO, chitosan, and Labrasol therefore provides a ternary nanoemulsion system with both improved stability and rapid antimicrobial activity, highlighting its potential for biomedical applications. These results support the potential of PAEO nanoemulsions as fast-acting antimicrobial systems suitable for biomedical or topical applications.

Keywords:
Essential oil; Nanoemulsion; Chitosan; Antibacterial; Antifungal; Physical stability.

1. INTRODUCTION

Essential oil from *Plectranthus amboinicus* (PAEO) has attracted considerable attention due to its antibacterial activity[1-3]. PAEO contains thymol and carvacrol, which exhibit efficacy against both gram-positive and gram-negative bacteria, and also drug-resistant strains like *Klebsiella pneumoniae* and MRSA [1, 2, 4, 5]. In detail, PAEO exhibits bactericidal effects via disrupting bacterial membranes, inhibiting efflux pump genes, and reducing biofilm formation [6, 7]. In the context of green chemistry and traditional medicine, PAEO shows potential as a safe and effective natural antimicrobial agent [3, 4, 6].

From a drug development perspective, the application of essential oils is limited by their hydrophobic nature, including volatility, poor aqueous solubility, and susceptibility to degradation [4]. These properties limit effective interactions with microbial cells, particularly in aqueous environments, resulting in inconsistent efficacy.

***Corresponding author:**
* Bao Ngoc Tran Email: baotn@hup.edu.vn

Furthermore, direct exposure of concentrated essential oils to skin or biological tissues can cause hypersensitivity or undesirable biointeractions [8-10]. To overcome these limitations, the development of biomaterial-based delivery systems capable of stabilizing essential oils while preserving their antimicrobial functionality is important for enabling reliable and reproducible bioactivity [11, 12]. In these delivery systems, essential oil is loaded into oily droplets that are dispersed in an aqueous continuous phase. These systems not only enhance the solubility of hydrophobic and volatile components but also improve the bioavailability and therapeutic efficacy of essential oil [5, 11].

In this study, PAEO was formulated as a nanoemulsion and evaluated for antibacterial activity against selected microbial strains. Nanoemulsions, typically consisting of droplets in the 20–200 nm range, provide a biocompatible and scalable platform for delivering lipophilic compounds [13-15]. Their large interfacial area promotes intimate contact between active ingredients and biological or microbial membranes, potentially enhancing antimicrobial efficacy and topical performance [14-16]. However, nanoemulsions are inherently thermodynamically unstable systems; therefore, careful optimization of surfactant and co-surfactant composition is essential to prevent droplet coalescence and maintain formulation stability [15, 17]. Here, this work employs a ternary phase diagram strategy to systematically explore the influence of surfactant, buffer, and chitosan composition on emulsion stability - an approach not commonly applied in essential oil formulation. Additionally, the study integrates the effects of co-solvent systems (ethanol with caprylocaproyl polyoxyl-8 glycerides (Labrasol) or dimethyl sulfoxide [DMSO]) in the oil phase to improve solubilization and enhance antimicrobial efficacy. This comprehensive design enables a deeper understanding of formulation parameters and their impact on droplet size and biological performance, providing a novel, structured methodology for developing effective and stable nanoemulsions for antimicrobial applications.

2. MATERIALS AND METHODS

2.1. Materials

PAEO was provided by Hanoi Natural Essential Oil Jsc. (Hanoi, Vietnam). The quality attributes of PAEO were provided in the Supplement data. Medium-chain triglyceride (MCT) oil, Chitosan (CS), polysorbate (Tween 80), absolute ethanol (EtOH), dimethyl sulfoxide (DMSO), Mueller-Hinton Broth (MHB), Tryptic Soy Agar (TSA), Sabouraud Dextrose (SD), and Sabouraud Dextrose Agar (SDA) were purchased from Merck SA (Merck KGaA, Darmstadt, Germany). Caprylocaproyl polyoxyl-8 glycerides (Labrasol) were gifted from Gattefossé (Saint-Priest, France). *Staphylococcus aureus* (ATCC 25923), *Escherichia coli* (ATCC 25922), *and Candida albicans (ATCC 10231)* were obtained from the FACM Laboratory at the Université Catholique de Louvain (Bruxelles, Belgium).

2.2. Methods

2.2.1. Nanoemulsion preparation

Nanoemulsions containing PAEO were prepared using a two-step dilution process. The first dilution phase (Phase 1) was prepared by dissolving 250 µL of 10% PAEO in either EtOH or MCT. The aqueous phase (Phase 2) comprised a mixture of the non-ionic surfactant Tween 80, Labrasol, ethanol (as cosolvent), chitosan solution at varying concentrations (0.1–5%, prepared in 1% acetic acid), and phosphate buffer (pH 7.4). The oil-to-aqueous phase ratio was optimized based on preliminary ternary phase screening.

The two phases were blended using a Benchmark D1000 programmable homogenizer (Benchmark Scientific, NJ, USA) fitted with a stainless-steel dispersing shaft. Homogenization was performed in 10 mL borosilicate glass tubes at 5000 rpm for 5 minutes at room temperature (25 °C) to obtain a coarse pre-emulsion. Immediately after homogenization, each formulation was visually inspected for clarity, phase separation, creaming, or flocculation to assess initial stability. Samples were stored at room temperature (25°C) in sealed containers protected from light and re-evaluated for macroscopic stability and phase integrity after 7 days.

2.2.2. Nanoemulsion physical characterizations

Microscopy observation

The appearance and physical stability of the essential oil emulsions were evaluated by visual inspection and optical microscopy after mounting the samples on glass slides and coverslips (Eclipse TE2000, Nikon, Tokyo, Japan). No staining or dilution was applied to preserve the native structure of the emulsion. The captured images were then analyzed using ImageJ software (NIH, USA). The histogram of droplet diameter distribution was plotted using OriginPro 2023 (OriginLab Corporation, USA). Optical microscopy was used only as a supportive morphological tool to evaluate visible droplet distribution, aggregation behavior, and phase homogeneity. Due to the optical resolution limit, such a small droplet (less than 5 µm diameter) could not be directly visualized by this technique. Therefore, droplet size measurements were primarily based on dynamic light scattering (DLS) rather than direct microscopic observation.

Dynamic light scattering

The average droplet size and size distribution of nanoemulsion formulations were determined using dynamic light scattering (DLS) with a Zetasizer Nano ZS90 (Malvern Panalytical, Malvern, UK). Measurements were conducted at 25 ± 0.5°C with a fixed detection angle of 173°. Before analysis, each sample was diluted 1:10 with deionized water to minimize multiple-scattering effects and ensure a count rate between 200 and 400 cps. The diluted samples were gently vortexed and equilibrated for 2 minutes before measurement. Instrument parameters were set with a dispersant refractive index of 1.330 and viscosity of 0.8872 cP (water), while the estimated refractive index of the oil phase was 1.45. Each sample was analyzed in triplicate. The results were expressed as intensity-based Z-average diameter (in nm) and polydispersity index (PDI). Samples showing PDI values greater than 0.3 were re-measured or excluded due to high polydispersity.

GC–MS analysis

The chemical compositions of the raw PAEO and final formulations were analyzed using a GC/MS-QP2020 system (Shimadzu, Japan) equipped with an SH-Rxi-5Sil MS capillary column. The raw PAEO was diluted in n-hexane (1:10) before analysis, and 1.0 µL of the diluted sample was injected into the GC–MS system. Helium was used as the carrier gas. The volatile constituents were identified by comparing their mass spectra and retention data with those in reference libraries. The relative composition of each component was expressed as the percentage peak area in the total ion chromatogram.

2.2.3. Determination of antimicrobial activity

The antimicrobial efficacy of nanoemulsion formulations containing PAEO was evaluated by determining the minimum inhibitory concentration (MIC) and minimum bactericidal concentration (MBC) against *Staphylococcus aureus* ATCC 25923, *Escherichia coli* ATCC 25922, and *Candida albicans* ATCC 10231. All strains were preserved at –80 °C and reactivated on appropriate agar media before testing.

The MIC and MBC values were determined following the broth microdilution method in accordance with Clinical and Laboratory Standards Institute (CLSI) guidelines. Briefly, nanoemulsion formulations and pure EO were serially diluted twofold in Mueller-Hinton Broth (MHB) for bacteria and Sabouraud dextrose broth (SDB) for yeast. A total of 100 µL of each concentration was transferred into the wells of 96-well plates.

Microbial suspensions were obtained from overnight cultures and adjusted to 0.5 McFarland standard (1.5×10^8 CFU/mL for bacteria, 1.5×10^6 CFU/mL for fungi), then diluted 1:100 in respective media to obtain the final working inoculum (1.5×10^6 CFU/mL for bacteria and 1.5×10^4 CFU/mL for fungi). 100 µL of this suspension was added to each well, resulting in a final volume of 200 µL per well. Plates were incubated at 37 °C for bacteria and 35 °C for fungi for 24 hours. The MIC was defined as the lowest concentration at which no visible turbidity was observed, indicating complete growth inhibition.

To determine MBC, 10 µL aliquots from all wells showing no visible growth were spot-inoculated onto Tryptic Soy Agar (TSA) for bacteria and Sabouraud Dextrose Agar (SDA) for *C. albicans*. After incubation at the appropriate temperature for 24 hours, the MBC was defined as the lowest concentration that resulted in a 99.9% reduction in colony count relative to the initial inoculum. All experiments were performed in triplicate, and two independent experiments confirmed the results.

The killing efficacy at a short exposure time (30 seconds) was also evaluated, and the microbial changes were reported as log reductions (Δlog10). Stock cultures and working suspensions were prepared in an appropriate sterile diluent as mentioned above. Equal volumes (1:1, v/v) of the microbial suspension and the test formulation (500 µL each) were mixed and incubated for 30 seconds at room temperature. After exposure, the mixture was promptly diluted in phosphate-buffered saline (PBS) to neutralize residual antimicrobial activity. Serial dilutions were plated on appropriate agar media, incubated under standard conditions, and viable colony-forming units (CFUs) were enumerated. The results were expressed as log reduction ($\Delta\log_{10}$) in CFU compared to the initial inoculum.

2.2.4. Data analysis

Mean values and standard deviations of particle size (Z-avg) and polydispersity index (PDI) were analyzed. Ternary diagrams were prepared using TernaryPlot.com. MIC, MBC data, and statistical analysis were conducted using one-way ANOVA in GraphPad Prism (version 7.1, Boston, MA, USA).

3. RESULTS

3.1. Nanoemulsion formulation: Screening phase 1

The target nanoemulsions were created using a two-step dilution process: Phase 1 was prepared by dissolving PAEO in various solvents to form a homogeneous solution before Phase 2. In Phase 1, EtOH

Table 1. Preliminary formulation design and stability results.

Formulation	Phase (1)	Phase (2)	Appearance (after 5 min)	Appearance (after 7 days)
F1.1	10% PAEO Ethanol	Ethanol 10%	-	-
F1.2		Ethanol 25%	x	-
F1.3		Ethanol 50%	x	x
F1.4		Ethanol 75%	x	x
F1.5		CS 0.1%	-	-
F1.6		CS 0.5%	-	-
F1.7		CS 1%	x	-
F1.8		CS 5%	x	x
F2.1	10% PAEO in MCT	Ethanol 10%	x	-
F2.2		Ethanol 25%	x	-
F2.3		Ethanol 50%	x	-
F2.4		Ethanol 75%	x	x
F2.5		CS 0.1%	-	-
F2.6		CS 0.5%	-	-
F2.7		CS 1%	x	x
F2.8		CS 5%	x	x

"CS": the solution of chitosan (CS), prepared in acetic acid 1 % solution.
"x" homogeneous appearance
"-": sediment or phase separation occurred

was used as a hydrophilic solvent, and MCT as a hydrophobic solvent. After dispersing Phase 1 into Phase 2, homogeneous dispersion systems were recorded, as indicated by the "x" and "green" shading in Table 1.

As shown, formulations containing 50–75% ethanol (F1.3, F1.4, F2.3, and F2.4) remained homogeneous after 5 min. In particular, F1.3 and F1.4 produced translucent and physically stable emulsions (Figure 1A). In contrast, formulations containing lower ethanol concentrations (10–25%) or low chitosan contents (≤0.5%) exhibited phase separation during storage. Representative examples of homogeneous, sedimented, and creamed emulsions are shown in Figure 1A. In Figure 1 B- E, optical microscopy revealed rapid changes in droplet size distribution within the first 5 min after preparation. Therefore, preliminary screening was based primarily on visual assessment of homogeneity and phase separation. The improved stability at higher ethanol concentrations may be attributed to reduced interfacial tension between the oil and aqueous phases, facilitating droplet formation and limiting coalescence [16]. CS, a cationic biopolymer, can stabilize emulsions through electrostatic repulsion and increased viscosity of the continuous phase, thereby reducing droplet aggregation and coalescence [18, 19]. Based on these results, ethanol and chitosan were identified as critical parameters and were further investigated using ternary phase diagrams.

3.2. Nanoemulsion formulation development

The ternary phase diagrams (Figure 2A–D) summarized the emulsification outcomes of various combinations of aqueous phase components: Tween 80 at the concentration of 3% (A), phosphate buffer at pH 7.4 (B1), and 1% chitosan solution (C), used to dilute a fixed oil phase of 10% PAEO in EtOH. Each point in the diagrams represented a specific A: B1:C ratio, with the total equal to 100%. The phase behavior of each formulation was visually assessed and categorized into three outcomes: homogeneous emulsion (green), oil precipitation at the bottom (blue), and oil layer separation at the surface (orange). Figure 2A illustrates the formulations exhibiting homogeneous dispersion, which is concentrated primarily in the region with a high A content (≥ 50%). This again indicated that Tween 80 plays a dominant role in stabilizing the oil droplets by lowering interfacial tension and increasing steric hindrance between droplets. As shown in Figure 2B, formulations containing high proportions of phase C (>75%) exhibited phase separation, characterized by oil accumulation at the surface. This behavior may be attributed to the increased viscosity of the continuous phase and insufficient surfactant coverage at the oil–water interface, resulting in oily accumulation onto the surface. Conversely, Figure 2C showed the region where formulations led to precipitation of the oil phase. This occurred when the phosphate buffer (B1) dominated the composition and the surfactant level was suboptimal (A < 25%). Finally, Figure *2*D, which overlaid all three phase behaviors, highlighted a key finding: the balance among sufficient surfactant (A), moderate ionic strength from the phosphate buffer (B), and polymeric stabilization by chitosan (C) is critical for forming and maintaining stable emulsions. Notably, the green region (homogeneous zone) formed a corridor adjacent to the

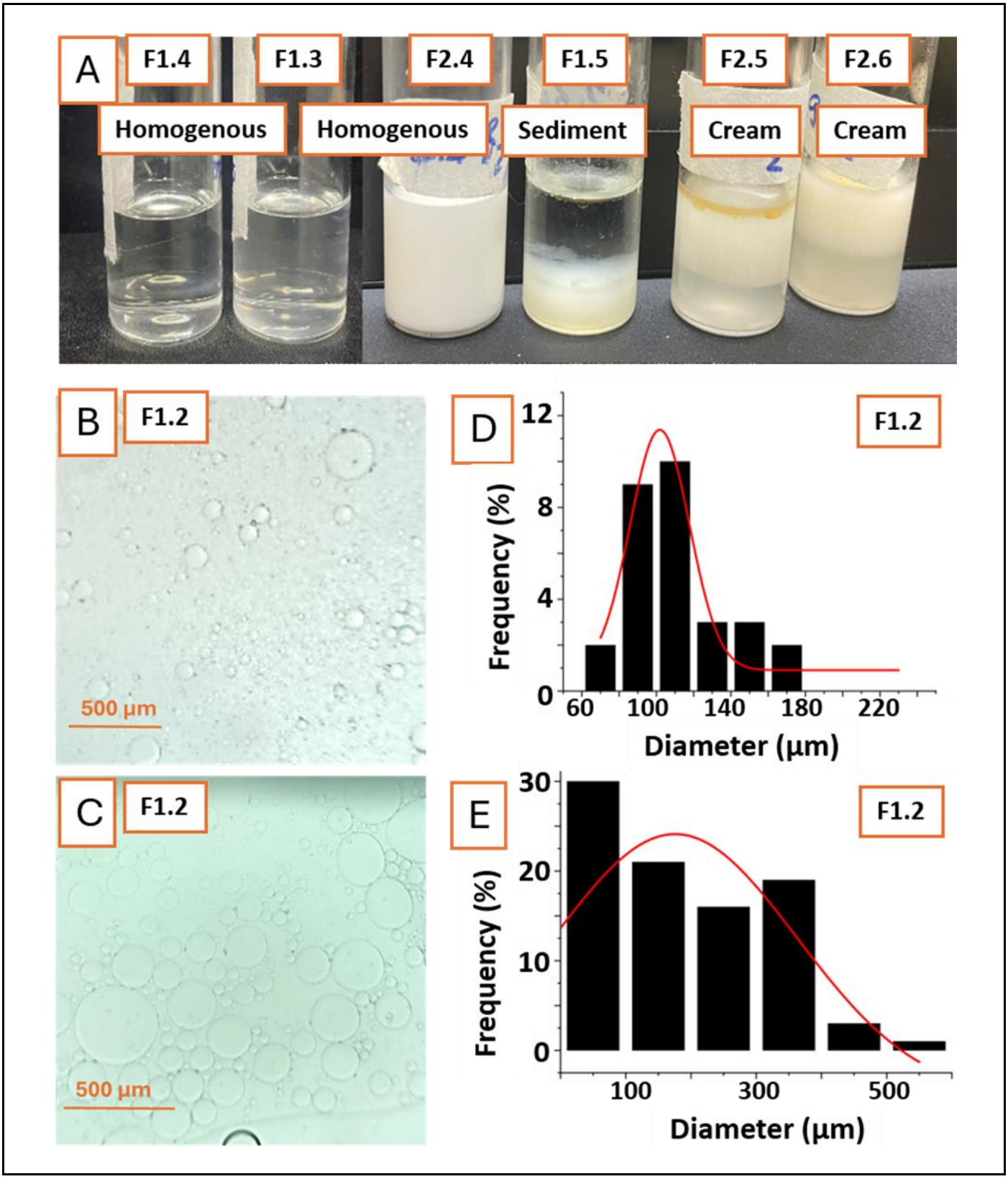

Figure 1. Physical appearance and droplet characteristics of representative PAEO emulsions. (A) Representative homogeneous formulations, including F1.3 and F1.4 containing high ethanol concentrations and F2.4 containing a lower ethanol concentration, a sedimented formulation (F1.5) and creamed formulations (F2.5 and F2.6). (B, D) Optical micrograph and corresponding droplet size distribution of formulation F1.2 immediately after preparation (t = 0 min). (C, E) Micrograph and droplet size distribution of the same formulation after 5 min of storage (t = 5 min). Scale bar = 500 µm.

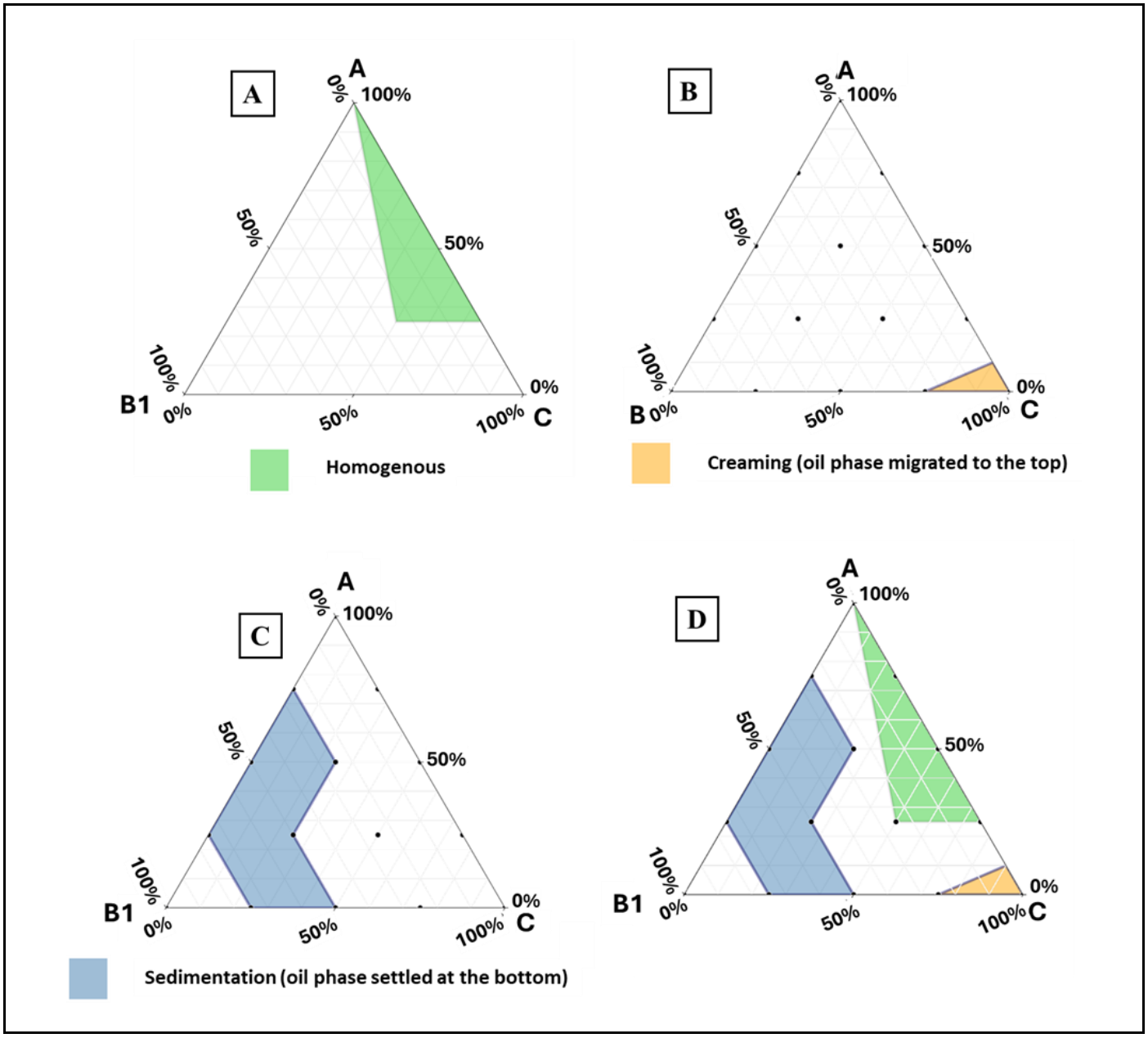

Figure 2. Ternary phase diagrams of PAEO emulsion systems composed of Tween 80 (A), phosphate buffer pH 7.4 (B1), and 1% chitosan solution (C). Ternary phase diagrams show (2A): homogeneous formulations (green region), (2B): creaming behavior (orange region), indicating migration of the oil phase to the upper layer, (2C): sedimentation behavior (blue region), indicating settling of the oil phase to the bottom layer, and (2D): overlay diagram summarizing the homogeneous, creaming, and sedimentation regions.

blue and orange zones, suggesting a narrow window for optimal nanoemulsion stability. These diagrams provided visual guidance for selecting promising formulations and underscored the synergistic interactions among surfactants, buffers, and polymers in stabilizing essential oil-based nanoemulsions.

3.3. Effect of incorporating Labrasol on emulsion properties

To further enhance emulsion performance, Labrasol, a well-known PEG-8 caprylic/capric glyceride surfactant, was added to the aqueous Phase 2 (B2, Figure 3). Upon incorporation of Labrasol (B2), the updated ternary phase diagrams (Figure 3) exhibited three distinct physical regions: creaming (orange), sedimentation (blue), and homogeneous (green).

Figure 3A showed that the inclusion of Labrasol expanded the green (homogeneous) region larger than Figure 2A. This suggested a synergistic stabilizing effect between Tween and Labrasol. Compared with Figure 2B, the creaming region in Figure 3B remained confined to formulations containing high chitosan contents and low surfactant levels. Figure 3C indicates that the addition of Labrasol was insufficient to eliminate sedimentation. While creaming was mainly associated

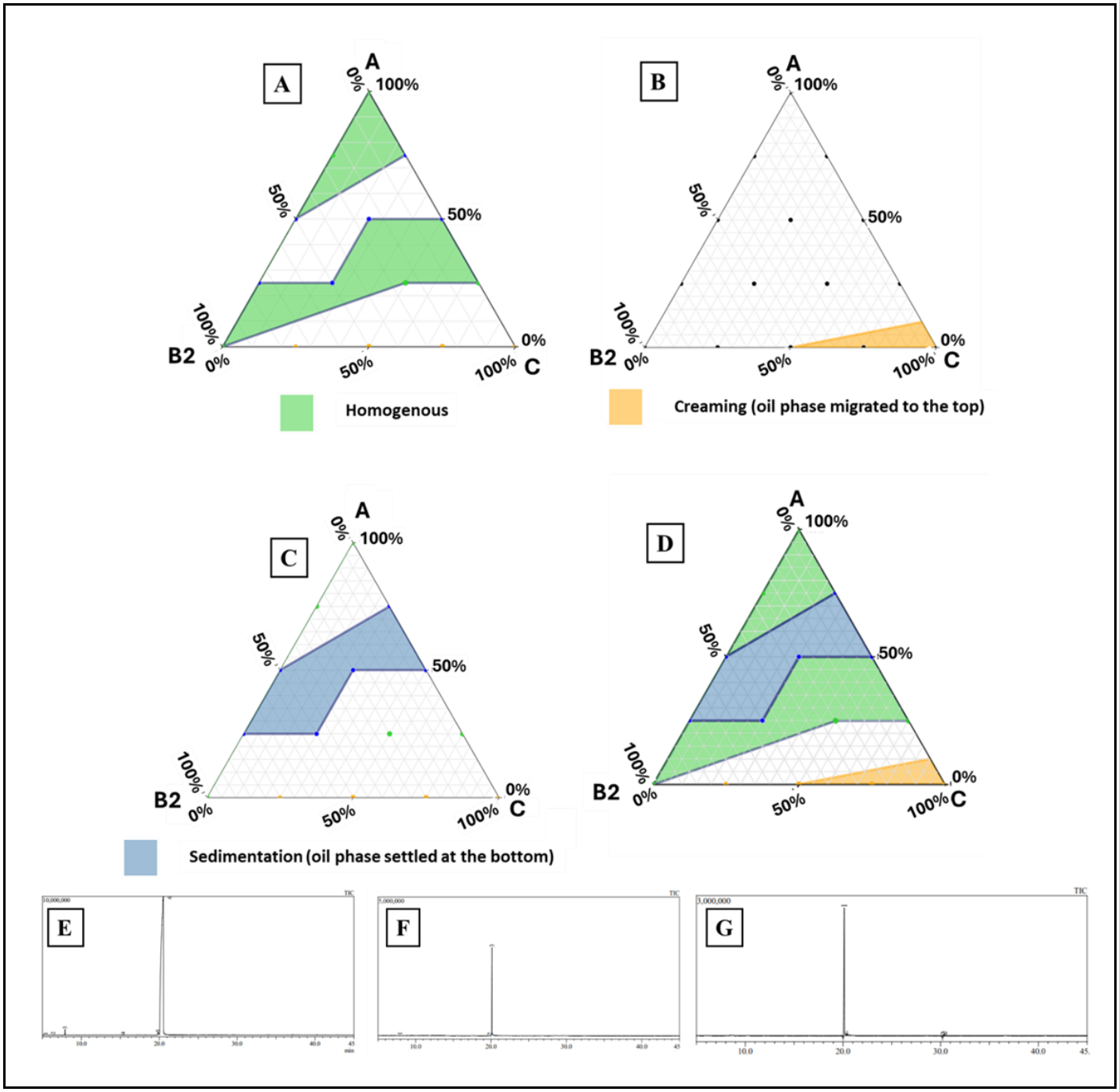

Figure 3. Ternary phase diagrams of PAEO composed of Tween 80 (A), phosphate buffer pH 7.4 containing 1% Labrasol (B2), and 1% chitosan solution (C). Ternary phase diagrams show (3A): homogeneous formulations (green region), (3B): creaming behavior (orange region), indicating migration of the oil phase to the upper layer, (3C): sedimentation behavior (blue region), indicating settling of the oil phase to the bottom layer, and (3D): overlay diagram summarizing the homogeneous, creaming, and sedimentation regions. (3E-G): GC-MS analysis of raw PAEO, F16, and F25 in Table 2.

Table 2 shows the droplet size and physical stability of representative formulations selected from the ternary phase diagrams. Formulations prepared without Labrasol (B1 group) exhibited droplet sizes ranging from 184 nm to over 2100 nm. Among them, the formulation containing 100% Tween 80 (Sample 1) produced the smallest droplets (Z-average: 184 ± 1 nm, PDI: 0.38 ± 0.01), demonstrating the strong emulsifying capability of Tween 80 alone. Additionally, several formulations produced droplets smaller than 500 nm, including formulation 10 (a more complex ternary system containing all three A-B1-C ingredients).

GC-MS analysis revealed several volatile constituents, including α-pinene, β-pinene, o-cymene, thymol, and carvacrol, as the predominant components (Figure 3E-G, Table 3). In two selected nanoemulsion formulations (F16 and F25 in Table 2), GC-MS analysis was conducted after 1 week of storage. The results showed that carvacrol remained the major detected peak, indicating that the principal volatile marker of PAEO

Table 2. Ternary formulation and characterization of PAEO nanoemulsions**.**

	Composition (%)			Appearance			After 24 h		After 7 days	
No.	**A**	**B1**	**C**	**Homo.**	**Cream.**	**Sed.**	**Z-avg (nm)**	**PDI**	**Z-avg (nm)**	**PDI**
F1	100	0	0	x			184 ± 1	0.3*8* ±0.01	249 ± 7	0.34 ±0.03
F2	75	25	0			X				
F3	50	50	0			X				
F4	25	75	0			x				
F5	0	100	0							
F6	0	75	25			X				
F7	0	50	50			X				
F8	0	25	75		x					
F9	0	0	100		x					
F10	25	25	50	x			323 ± 1	0.27 ± 0.04	315 ± 1	0.32 ± 0.04
F11	25	50	25			X				
F12	50	25	25			X				
F13	25	0	75	x			2102 ±5	0.10 ±0.02		
F14	50	0	50	x		X	1298 ±2	0.2*5* ±0.04		
F15	75	0	25	x		X	1148 ±3	0.19 ±0.03		
No.	**A**	**B2**	**C**	**Homo.**	**Cream.**	**Sed.**	**Z (nm)**	**PDI**	**Z (nm)**	**PDI**
F16	100	0	0	x			181 ±2	0.22 ±0.01	177 ± 3	0.22 ±0.04
F17	75	25	0	x			298 ±1	0.25 ± 0.05		
F18	50	50	0			x				
F19	25	75	0			x				
F20	0	100	0	x			353 ± 5	0.16 ± 0.02		
F21	0	75	25			x				
F22	0	50	50		x					
F23	0	25	75		x					
F24	0	0	100		x					
F25	25	25	50	x			908 ± 8	0.26 ± 0.06	1171 ± 12	0.15 ± 0.02
F26	25	50	25			x				
F27	50	25	25			x				
F28	25	0	75	x			2102 ± 3	0.10 ± 0.03		
F29	50	0	50			x				
F30	75	0	25			x				

A: Tween 80; B1: phosphate buffer pH 7.4; B2: phosphate buffer pH 7.4 containing 1% Labrasol; C: 1% chitosan solution. “Homo”: homogeneous appearance; “Cream”: phase separation, oil phase migration to the top; “Sed.”: phase separation, oil phase accumulation at the bottom. Data are presented as mean ± SD (n = 3).

was retained after formulation. However, it should be noted that the current GC-MS data are primarily qualitative and semi-quantitative, based on relative peak areas, and did not provide absolute quantification of PAEO content. As this study was intended to evaluate the feasibility of PAEO-based nanoemulsions in antibacterial models, a quantitative determination of the PAEO content was not performed.

After preliminary screening, two representative formulations, F16 and F25 (Table 2), were selected for further investigation. To evalute the individual effects of Labrasol and chitosan, four (04) formulations were evaluated: F1-3 (F16; without Labrasol and chitosan), F2-3 (F16 supplemented with Labrasol), F1-4 (F16 supplemented with chitosan), and F2-4 (F25; containing both Labrasol and chitosan). This design aims to systematically assess the effects of Labrasol, chitosan, and their combination.

3.4. Microbiological activities

3.4.1. Antibacterial effects of pure PAEO

As shown in the MIC experiment (Figure 4A and Figure 4C), raw PAEO exhibited inhibitory activity against all tested strains, but with a large standard deviation. For *S. aureus*, the PAEO’s MIC values ranged from 0.0156 to 0.125 %, highlighting an 8-fold variability. Similarly, against *E. coli* and *C. albicans*, PAEO showed MIC ranges of 0.025–0.5% and 0.125–0.5%, respectively. These variable results might be due to the physical properties of PAEO, which made

Table 3. GC-MS analysis results of raw PAEO, F16 and F25 in Table 2.

Compound	Retention time (min)	Raw PAEO (%)	F16 (%)	F25 (%)
α-Pinene	5.14	0.03	–	–
β-Pinene	6.38	0.03	–	–
o-Cymene	7.90	0.54	0.28	–
Estragole	15.37	0.07	–	–
Thymol	19.83	0.86	0.25	–
Carvacrol	20.53	98.48	99.47	99.53
Unknown/others	30.34	–	–	0.47
Total		100.00	100.00	100.00

Percent (%) was calculated based on relative peak area.

it difficult to obtain a homogeneous dispersion for consistent activity. Therefore, the formulation of the PAEO-emulsified system aimed to achieve more consistent antimicrobial effects and enhance its practical applicability.

3.4.2. Bactericidal and fungicidal efficacy of PAEO nanoemulsion formulations

To ensure that the biological activity was associated with the formulation design, excipients were tested for antibacterial activity. Tween 80 (A) and phosphate buffer systems (B1/B2) showed no detectable MIC under the tested conditions. Chitosan solution prepared in acetic acid (C) showed antibacterial effects (0.125 mg/mL); however, this activity was diminished after pH adjustment to the range of 6.0 to 7.0. In the final PAEO formulations, chitosan was incorporated into buffered systems. Moreover, ethanol in the formulation was highly diluted in the antibacterial assays and was well below the reported antimicrobial range (20–22%). Therefore, the observed antibacterial activity was more likely associated with the combined formulation system, particularly the PAEO effect.

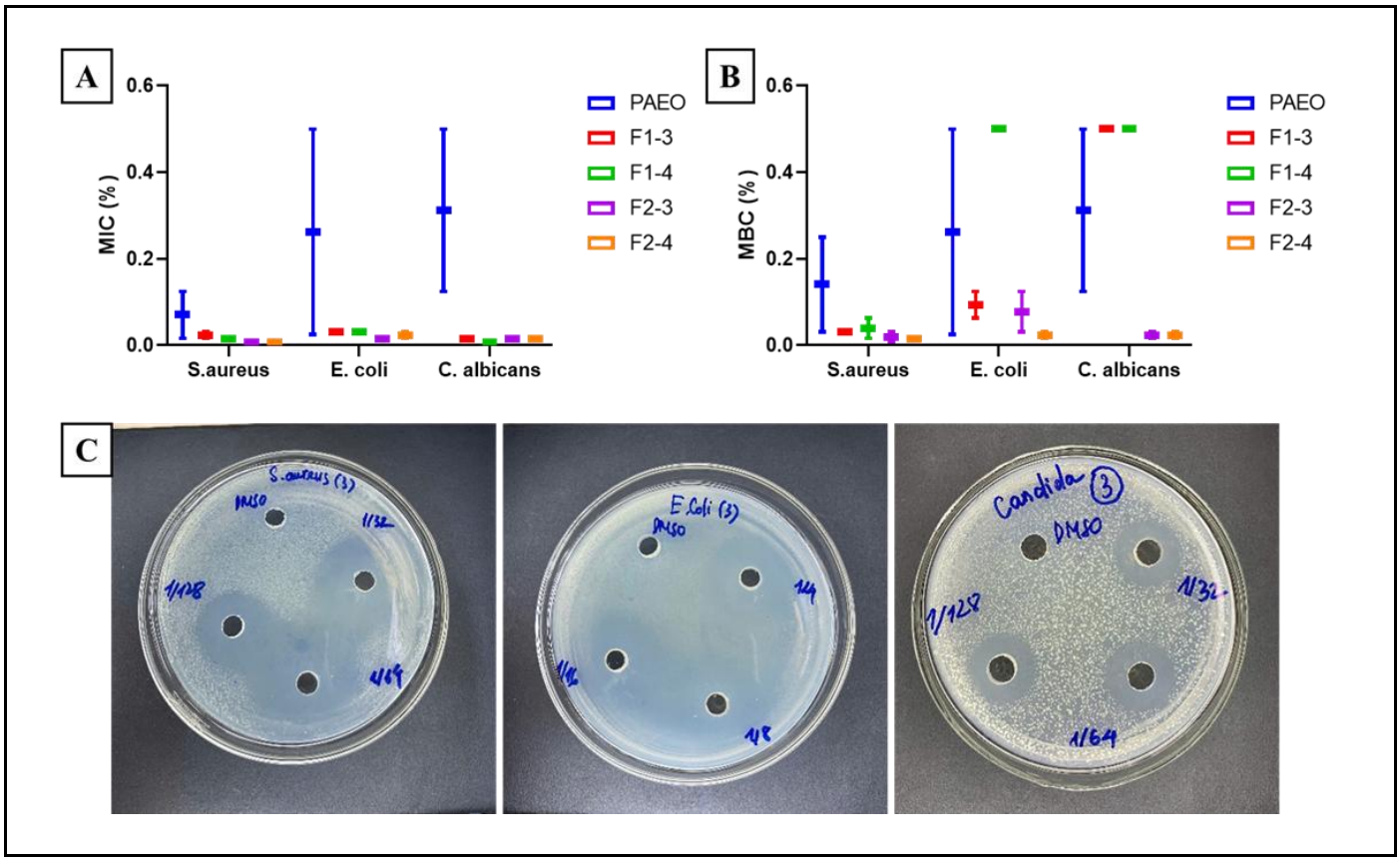

Figure 4. (A) MIC and (B) MBC of pure PAEO and nano-emulsion formulations, (C) representative images for PAEO antimicrobial activity against gram-positive (*Staphylococcus aureus*), gram-negative (*Escherichia coli*) bacteria, and yeast (*Candida albicans*).

Upon formulation into nanoemulsions, the antimicrobial effect became more consistent and, in many cases, significantly enhanced. All tested formulations (F1-3, F1-4, F2-3, and F2-4) exhibited lower, narrower MIC values against microbial strains than PAEO (Figure 4A). Among them, formulation F2-4 consistently demonstrated the lowest MIC values, particularly against *S. aureus* and *E. coli* (approximately 0.015- 0.031%). Similar trends were observed in the MBC results (Figure 4B). While native PAEO exhibited broad MBC values (up to 0.5 %), the nanoformulations notably reduced these thresholds. F2-4 again emerged as the most effective formulation, showing the lowest MBC values across all tested strains. ANOVA results indicated a statistically significant difference in MIC values among the tested groups ($p = 0.0087$); the multiple comparisons test showed that all tested nanoemulsion formulations were significantly different from raw PAEO ($p < 0.01$).

These results emphasized the crucial role of formulation design. The incorporation of Labrasol in Phase 1 appeared to enhance essential oil solubilization and permeability, likely facilitating better interactions with microbial membranes. Additionally, the ternary aqueous system (Tween 80, phosphate buffer, and 1% chitosan) in Phase 2 improved emulsion stability and further enhanced antimicrobial effects. Notably, formulations containing both Labrasol and the ternary aqueous system (F2-4) showed the strongest and most consistent performance, suggesting synergistic effects between the components. Collectively, these findings validated the potential of nanoemulsion technology to improve the stability and antimicrobial performance of essential oils and supported F2-4 as a promising candidate for practical antimicrobial applications.

3.4.3. Bactericidal and fungicidal efficacy of nanoemulsion in short-time exposure

The antimicrobial activities of nanoemulsion formulations were further confirmed through log CFU reduction assays, with results summarized in Figure 5. Microbial counts after 30 seconds of exposure to the formulations were compared to initial inoculum levels. The dotted line at -3 Δlog CFU represented the threshold for a 99.9% reduction in viable microorganisms. F1-4 and F2-4 demonstrated significant bactericidal and fungicidal effects, achieving ≥ 3-log reductions (equivalent to ≥99.9% killing efficiency) across all tested strains, including *Staphylococcus aureus*, *Escherichia coli*, and *Candida albicans*. These results validated the enhanced bioactivity of the nanoemulsion systems, particularly those containing the ternary surfactant mixture (Tween 80, Labrasol®, and chitosan solution), which likely contributed to improved solubilization and cellular penetration of PAEO. The rapid and consistent microbial reduction observed with the optimized emulsions confirmed their potential as stable, effective carriers of PAEO for topical antimicrobial applications.

4. DISCUSSION

The PAEO has demonstrated significant antibacterial efficacy in previous studies [1, 4]. However, the variability in MIC and MBC values in microbial experiments (higher MIC values and an 8-fold difference in MIC for *S. aureus* or *E. coli*) suggested inconsistencies in performance. Our current study hypothesized that this limitation was due to the hydrophobicity of essential oils. Therefore, a suitable nanoemulsion can improve oil dispersion and ensure

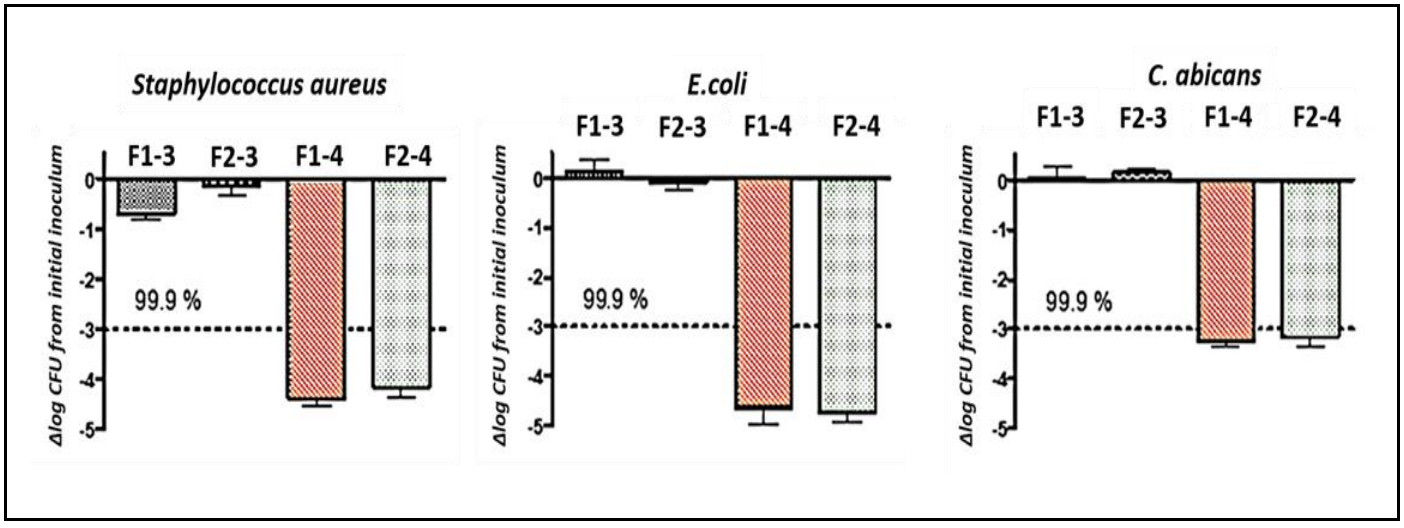

Figure 5. Microbial counts after 30 seconds of exposure to the formulations were compared to initial inoculum levels.

ensure consistent antibacterial activity. In fact, all nanoemulsion formulations exhibited markedly lower MIC and MBC values than pure PAEO. Statistical analysis confirmed significant differences between PAEO and all tested emulsions. Specifically, combining ternary surfactant systems in formulation F1-4 and F2-4 consistently achieved >99.9% microbial reduction across all tested strains (*S. aureus*, *E. coli*, and *C. albicans*) within 30 seconds of exposure, indicating a rapid bactericidal effect [20, 21]. It should be noted that this study was preliminary and focused on evaluating the feasibility of PAEO-based nanoemulsions for antibacterial applications. The intended application of the developed nanoemulsion system is topical delivery; it can be extended to mucosal surfaces, such as mouthwash or other topical applications [1, 22]. This positioning was supported by the rapid antimicrobial activity observed in the present study (within 30 seconds), which is consistent with typical contact times in oral hygiene applications. In addition, compared with previous studies that used a high proportion of Tween or organic solvents [22, 23], nanoemulsions are well suited for use in the oral cavity because they can disperse lipophilic essential oils in aqueous media and enhance their activity against microbial biofilms. The current formulation is not intended as a final dosage form, and further studies, including evaluation of mucosal compatibility, safety, and formulation optimization, are required to confirm its suitability for potential clinical use.

The use of ternary phase diagrams in this study provided an effective and visual approach to map emulsion behavior across varying component ratios, specifically Tween 80 (surfactant), phosphate buffer at pH 7.4 (aqueous phase), and CS solution (polymeric stabilizer). This design allowed us to identify regions corresponding to homogeneous emulsions, as well as formulations exhibiting creaming or sedimentation. Unlike self-nanoemulsifying drug delivery systems (SNEDDs) studies [23, 24], our approach prioritized the fine mapping of component interactions using discrete experimental points rather than continuous titration [25]. Compared to self-microemulsifying drug delivery systems (SMEDDs) or SNEDDs, which typically emphasize the role of co-solvents and co-surfactants [25, 26], our method incorporated a pH-dependent polymeric stabilizer (chitosan) and focused on the physical stability and reproducibility of the resulting emulsion systems.

In this study, several formulations exhibited mean droplet sizes exceeding 200 nm, while some preliminary systems approached the micrometer range. These values exceed the conventional nanoemulsion size range (typically 20 – 200 nm) [14, 16]. However, the upper size limit of nanoemulsions can be extended to approximately 500 nm in some classifications depending on formulation composition, surfactant concentration, and interfacial stabilization mechanisms [17, 27]. Nanoemulsions are generally regarded as stable colloidal dispersions that require external energy input for formation. In contrast, microemulsions are thermodynamically stable, isotropic systems that form spontaneously in the presence of surfactants and co-surfactants [15]. In contrast, the term “nanoscale materials” represents a broader dimensional or regulatory concept and should not be used interchangeably with the term “nanoemulsion” [28]. Accordingly, the obtained formulations with droplet sizes below 500 nm were discussed as nanoscale emulsion systems from both colloidal and formulation perspectives, whereas systems approaching or exceeding 1 μm were more appropriately categorized as coarse or macroemulsions. This terminology provides a more pharmaceutical classification of the colloidal systems investigated.

Based on our observations, Tween, chitosan, and Labrasol played complementary roles in the final nanoemulsion formulation. To further interpret the observed formulation behavior, a risk-based assessment of the key ingredients was conducted to summarize their impacts (direct or indirect) on critical attributes, such as droplet size and physical stability (Table 4). Chitosan, a biocompatible and biodegradable polysaccharide, contributes to formulation stability through its viscosity-enhancing and mucoadhesive properties [29-31]. These characteristics help prolong the residence time of the nanoemulsion at the target site, potentially enhancing local therapeutic effects [30, 32, 33]. Chitosan may exert intrinsic antimicrobial activity [18, 29, 32]; however, at neutral pH (when combining three phases), the effects of the placebo samples were undetectable. Here, chitosan was used solely as a carrier excipient [31, 34]. Compared to conventional chitosan-coating strategies, the pH-dependent property of chitosan was utilized *in situ*. During emulsification, the addition of an alkaline buffer (B) modulated the system's viscosity and interfacial architecture, thereby enhancing kinetic stability and promoting the formation of uniform nanoemulsion droplets. The antibacterial activity was primarily attributed to PAEO, as placebo components (Tween 80, buffer systems, chitosan, and diluted ethanol) exhibited minimal or undetectable antimicrobial effects.

Labrasol (caprylocaproyl macrogol-8 glyceride) is a nonionic surfactant widely used in pharmaceutical formulations [18, 35]. Labrasol inclusion in the oil phase enhances emulsification efficiency and droplet dispersion, promoting better penetration and bioavailability [35]. Importantly, both chitosan and Labrasol are recognized for their favorable safety profiles [36]. Chitosan has been extensively evaluated in biomedical applications and is well tolerated on skin and mucosal surfaces.

Table 4. Formulation rationale and proposed risk assessment.

Ingredient	Process steps	Main role in formulation	Impact on particle size	Impact on physical stability	Mechanistic rationale
Ethanol	Phase 1	Co-solvent	Medium	Medium	Enhances mutual miscibility between oil and aqueous phases, facilitating droplet formation. However, excessive ethanol may weaken the interfacial film and reduce stability.
MCT oil	Phase 1	Oil phase; dilution oils	Medium	Strong & Negative	Oil content strongly influences droplet size; higher oil loading typically requires more surfactant, otherwise leading to droplet growth and instability. (Table 1)
Tween 80	Phase 2	Primary surfactant	Strong	Strong	Controls droplet breakup and interfacial coverage. Adequate surfactant levels lead to smaller droplets and improved resistance to phase separation.
Chitosan	Phase 2	Polymeric stabilizer; combining with B (phostphate buffer)	Strong	Strong	Enhances stability by increasing continuous-phase viscosity and providing electrostatic repulsion. Excess chitosan may increase droplet size or induce aggregation (bridging flocculation).
Phosphate buffer (pH 7.4)	Phase 2	pH adjustment	Low	Medium	Limited direct effect on droplet formation, but influences stability via ionic strength and chitosan ionization, affecting interfacial interactions.
Labrasol	Phase 2	Co-surfactant;	Medium–Strong	Medium–Strong	Reduces interfacial tension and increases interfacial fluidity, facilitating formation of smaller droplets and expanding the homogeneous region in the ternary phase diagram.

Labrasol is classified as a generally recognized as safe (GRAS) excipient and is commonly used in oral and topical formulations without reported adverse effects [37]. Together, these excipients contribute not only to the physicochemical performance of nanoemulsion but also to its suitability for future antimicrobial therapies. However, stable regions are only observed in the presence of sufficient surfactants, suggesting that chitosan acts as a co-stabilizer rather than a primary emulsifying agent.

As a limitation of this study, the term "stable" was used only to describe the preliminary results, in which the short-term stable PAEO emulsions were considered suitable for antibacterial evaluation (requiring 24 – 48 h incubation). Further formulation development may require additional excipients depending on the intended dosage form and route of administration, which could influence the physicochemical properties and stability behavior of the systems. Therefore, comprehensive quantitative and longitudinal stability studies were not performed in the current work and will be investigated in future studies.

5. CONCLUSION

This research introduced a formulation strategy for essential oil nanoemulsions, employing ternary phase diagrams and particle-size analysis to identify short-term stable, homogeneous systems. The optimized emulsions, which included surfactant, buffer, and chitosan, demonstrated enhanced physical properties and uniform droplet size distributions. *In vitro* antimicrobial results indicated that the obtained emulsions improved inhibitory effects against *S. aureus, E. coli,* and *C. albicans*. These results are promising for additional research to confirm the clinical significance of these formulations.

6. ACKNOWLEDGEMENT

The authors thank local suppliers and laboratories for providing the certificate of analysis for *Plectranthus amboinicus* essential oil (PAEO). The authors thank Sapharchem, Vietnam, for providing the samples from Gattefossé. This study project does not have specific funding. This research was conducted as part of the academic and community initiative activities at the Hanoi University of Pharmacy.

Author contribution

Khanh Ngoc Le: investigation, methodology, data curation, writing – review & editing

Dang Le Hai Hoang, Quang The Nguyen, Thanh Tien Nguyen, Anh Nam La, Dung Phuoc Tran Nguyen, Ngan

Bao Hoang: conceptualization & investigation, these authors contributed equally.
Quynh Nhu Thi Nguyen, Nhung Mai-Hong Nguyen: investigation, methodology, supervision, writing – original draft.
Bao Ngoc Tran: investigation, methodology, conceptualization, data curation, writing - original draft preparation, writing – review & editing

Funding
This research did not receive any specific grant from funding agencies.

Conflict of interest
The authors do not have any conflicts of interest to disclose

Ethics approval
Not applicable. This study did not involve human participants or live animals requiring ethical approval.

Article info:
Received January 18, 2026
Received in revised form June 1, 2026
Accepted June 19, 2026

REFERENCES

1. Arumugam G, Swamy MK, Sinniah UR. *Plectranthus amboinicus* (Lour.) Spreng: Botanical, phytochemical, pharmacological and nutritional significance. Molecules. 2016;21(4):369.
2. Sandner G, Heckmann M, Weghuber J. Immunomodulatory activities of selected essential oils. Biomolecules. 2020;10(8):1139.
3. Nandini K, Shruthi G, Sindhu TS, Vedashree PN, Archer AC. Bio-functional nanoemulsion of *Plectranthus amboinicus* essential oil: Molecular insights into obesity control. Food Chem Adv. 2025;8:101063.
4. Santos Filipe M, Bangay G, Brauning FZ, Ogungbemiro FO, Palma BB, Díaz-Lanza AM, et al. *Plectranthus amboinicus*: A systematic review of traditional uses, phytochemical properties, and therapeutic applications. Pharmaceuticals. 2025;18(5):707.
5. Vijayakumar S, Vinoj G, Malaikozhundan B, Shanthi S, Vaseeharan B. Plectranthus amboinicus leaf extract mediated synthesis of zinc oxide nanoparticles and its control of methicillin resistant *Staphylococcus aureus* biofilm and blood sucking mosquito larvae. Spectrochim Acta A Mol Biomol Spectrosc. 2015;137:886-91.
6. Gonçalves TB, Braga MA, de Oliveira FF, Santiago GM, Carvalho CB, Brito e Cabral P, et al. Effect of subinihibitory and inhibitory concentrations of *Plectranthus amboinicus* (Lour.) Spreng essential oil on *Klebsiella pneumoniae*. Phytomedicine. 2012;19(11):962-8.m.
7. Augustus AR, Jana S, Samsudeen MB, Nagaiah HP, Shunmugiah KP. *In vitro* and *in vivo* evaluation of the anti-infective potential of the essential oil extracted from the leaves of *Plectranthus amboinicus* (lour.) Spreng against *Klebsiella pneumoniae* and elucidation of its mechanism of action through proteomics approach. J Ethnopharmacol. 2024;330:118202.
8. Chang SL, Chang YC, Yang CH, Hong HS. Allergic contact dermatitis to *Plectranthus amboinicus* masquerading as chronic leg ulcer. Contact Dermat. 2005;53(6):356-7.
9. de Groot AC, Schmidt E. Essential oils, part IV: Contact allergy. Dermatitis. 2016;27(4):170-5.
10. Sindle A, Martin K. Art of prevention: Essential oils - Natural products not necessarily safe. Int J Womens Dermatol. 2021;7(3):304-8.
11. Yan C, Kim S-R, Ruiz DR, Farmer JR. Microencapsulation for food applications: A review. ACS Appl Bio Mater. 2022;5(12):5497-512.
12. Kim JH, Ko JA, Kim JT, Cha DS, Cho JH, Park HJ, et al. Preparation of a capsaicin-loaded nanoemulsion for improving skin penetration. J Agric Food Chem. 2014;62(3):725-32.
13. Garcia CR, Malik MH, Biswas S, Tam VH, Rumbaugh KP, Li W, et al. Nanoemulsion delivery systems for enhanced efficacy of antimicrobials and essential oils. Biomater Sci. 2022;10(3):633-53.
14. Harwansh RK, Deshmukh R, Rahman MA. Nanoemulsion: Promising nanocarrier system for delivery of herbal bioactives. J Drug Deliv Sci Technol. 2019;51:224-33.
15. McClements DJ. Nanoemulsions versus microemulsions: Terminology, differences, and similarities. Soft Matter. 2012;8(6):1719-29.
16. Shakeel F, Shafiq S, Haq N, Alanazi FK, Alsarra IA. Nanoemulsions as potential vehicles for transdermal and dermal delivery of hydrophobic compounds: An overview. Expert Opin Drug Deliv. 2012;9(8):953-74.
17. Su S, Lu J, Yin X, Wang M, Wang F, Pang Y. Encapsulation of β-carotene in chitosan Pickering nanoemulsion: Effect of process parameters and their stability. Food Chem. 2026;500:147505.
18. Ashkezari S, Abtahi MS, Sattari Z, Tavakkoli Yaraki M, Hosseini F, Inanloo Salehi R, et al. Antibiotic and inorganic nanoparticles co-loaded into carboxymethyl chitosan-functionalized niosome: Synergistic enhanced antibacterial and anti-biofilm activities. J Drug Deliv Sci Technol. 2023;83:104386.
19. Sable AA, Kunwar A, Barik A. Alginate and chitosan-based delivery systems for improving the bioavailability and therapeutic efficacy of curcumin. Pharmaceutics. 2024;16(3):423.
20. Nguyen TK, Argudín MA, Deplano A, Nhung PH, Nguyen HA, Tulkens PM, et al. Antibiotic resistance, biofilm formation, and intracellular survival as possible determinants of persistent or recurrent infections by *Staphylococcus aureus* in a Vietnamese tertiary hospital: Focus on bacterial response to moxifloxacin. Microb Drug Resist. 2020;26(6):537-44.
21. Peyrusson F, Varet H, Nguyen TK, Legendre R, Sismeiro O, Coppée JY, et al. Intracellular *Staphylococcus aureus* persisters upon antibiotic exposure. Nat Commun. 2020;11(1):2200.
22. Nazliniwaty N, Laila L. Formulation and antibacterial activity of *Plectranthus amboinicus* (Lour.) Spreng leaves ethanolic extract as herbal mouthwash against halitosis caused bacteria. Open Access Maced J Med Sci. 2019;7(22):3900.
23. Merchant J, Müllertz A, Rades T, Bannow J. Functionalized calcium carbonate (FCC) as a novel carrier to solidify supersaturated self-nanoemulsifying drug delivery systems (super-SNEDDS). Eur J Pharm Biopharm. 2023;193:198-207.
24. Priani SE, Nurhaliza A, Aryani R, Wilar G, Chaerunisaa AY, Sopyan I. Recent progress in supersaturation-based SNEDDS: Formulation, mechanism, and biopharmaceutical performance. OpenNano. 2025;25:100252.
25. Akhtar N, Mohammed SAA, Khan RA, Yusuf M, Singh V, Mohammed HA, et al. Self-Generating ano-emulsification techniques for alternatively-routed, bioavailability enhanced delivery, especially for anti-cancers, anti-diabetics, and miscellaneous drugs of natural, and synthetic origins. J Drug Deliv Sci Technol. 2020;58:101808.

26. Rumman M, Khan MV. Drug delivery systems for enhanced neuroprotective effects of polyphenols: Current status and challenges. J Drug Deliv Sci Technol. 2026;115:107767.
27. Jacob S, Kather FS, Boddu SHS, Shah J, Nair AB. Innovations in nanoemulsion technology: Enhancing drug delivery for oral, parenteral, and ophthalmic applications. Pharmaceutics. 2024;16(10):1333.
28. FDA. Considerations for Drug Products that Contain Nanomaterials. 2022.
29. Barbosa de Carvalho SY, Vieira SS, Kauany da silva Azevedo C, Leitão AA, Gustavo de Lima Guimarães L. Development and characterization of material resulting from the sulfation of chitosan incorporated with essential oils for application in the control of dermatophyte fungus. J Drug Deliv Sci Technol. 2024;102:106416.
30. dos Santos MK, Kreutz T, Danielli LJ, De Marchi JGB, Pippi B, Koester LS, et al. A chitosan hydrogel-thickened nanoemulsion containing *Pelargonium graveolens* essential oil for treatment of vaginal candidiasis. J Drug Deliv Sci Technol. 2020;56:101527.
31. Nguyen QM, Hutchison P, Palombo E, Yu A, Kingshott P. Antibiofilm activity of eugenol-loaded chitosan coatings against common medical-device-contaminating bacteria. ACS Appl Bio Mater. 2024;7(2):918-35.
32. Ghodsi R, Sadr Tahouri SK, Amjad F, Nasiri MR, Toutounchi A, Salehi H, et al. Chitosan/alginate@niosome-curcumin: High-performance wound dressing with enhanced antibacterial activity. J Drug Deliv Sci Technol. 2025;114:107438.
33. Nabil Y, Atta AH, El-Fattah WA, Hafez HS, Elshaarawy RFM. Progress in chitosan/essential oil/ZnO nanobiocomposites fabrication for wound healing applications: A review. Int J Biol Macromol. 2025;318(Pt 3):145123.
34. Sanuja S, Agalya A, Umapathy MJ. Studies on magnesium oxide reinforced chitosan bionanocomposite incorporated with clove oil for active food packaging application. Int J Polym Mater Polym Biomater. 2014;63(14):733-40.
35. Valizadeh H, Islambulchilar Z, Eskandarinia K, Zakeri-Milani P. Influence of oil phase surface properties on the physicochemical characteristics of meloxicam self-microemulsifying drug delivery systems. J Pharm Innov 2023;18(2):381-90.
36. Ding X, Zhao L, Khan IM, Yue L, Zhang Y, Wang Z. Emerging chitosan grafted essential oil components: A review on synthesis, characterization, and potential application. Carbohydr Polym. 2022;297:120011.
37. Burdock GA, Carabin IG. Generally recognized as safe (GRAS): History and description. Toxicol Lett. 2004;150(1):3-18.